



**HAL**  
open science

## Sea experimentation of single beacon simultaneous localization and communication for AUV navigation

Raphaël Garin, Pierre-Jean Bouvet, Philippe Forjonel, Beatrice Tomasi

► **To cite this version:**

Raphaël Garin, Pierre-Jean Bouvet, Philippe Forjonel, Beatrice Tomasi. Sea experimentation of single beacon simultaneous localization and communication for AUV navigation. OCEANS 2023, Jun 2023, Limerick, Ireland. hal-04132884

**HAL Id: hal-04132884**

**<https://hal.science/hal-04132884>**

Submitted on 19 Jun 2023

**HAL** is a multi-disciplinary open access archive for the deposit and dissemination of scientific research documents, whether they are published or not. The documents may come from teaching and research institutions in France or abroad, or from public or private research centers.

L'archive ouverte pluridisciplinaire **HAL**, est destinée au dépôt et à la diffusion de documents scientifiques de niveau recherche, publiés ou non, émanant des établissements d'enseignement et de recherche français ou étrangers, des laboratoires publics ou privés.

# Sea experimentation of single beacon simultaneous localization and communication for AUV navigation

Raphaël Garin  
*L@bISEN*  
*ISEN Yncréa Ouest*  
Brest, France  
raphael.garin@isen-ouest.yncrea.fr

Pierre-Jean Bouvet  
*L@bISEN*  
*ISEN Yncréa Ouest*  
Brest, France  
pierre-jean.bouvet@isen-ouest.yncrea.fr

Philippe Forjonel  
*L@bISEN*  
*ISEN Yncréa Ouest*  
Brest, France  
philippe.forjonel@isen-ouest.yncrea.fr

Beatrice Tomasi  
*Norce Research Center*  
*Norce Group*  
Bergen, Norway  
beto@norceresearch.no

**Abstract**—Autonomous underwater vehicles localization is a challenging task due to the harsh environment of the underwater propagation channel. To reach accurate positioning, it is often required to use either a complex architecture or costly sensors. In this paper we provide the experimental results of a cost-effective technique combining underwater acoustic communication and localization through Doppler shift estimation that provides information on receiver relative speed. We consider a fixed anchor with known position transmitting regularly to a moving boat in water at a constant depth of 2 meters in a range up to 800 meters. Using an Extended Kalman filter, we compare standalone range measurements estimation with speed and range combined in the estimation filter. Experimental results demonstrate a consequent gain using speed computation associated with range measurement and a good accuracy on positioning results.

**Index Terms**—Underwater navigation, EKF, underwater acoustic communications, Doppler shift estimation, Autonomous underwater vehicle.

## I. INTRODUCTION AND MOTIVATIONS

Autonomous underwater vehicles are self-propelled vehicles designed for missions without any human intervention. They have been developed since the early 1970s and are nowadays intensively exploited to perform tasks previously made by manned vehicles. They are used in a variety of applications, such as marine science, offshore oil and gas exploration, military operations, and underwater surveillance. The Autonomous Underwater Vehicle (AUV) navigation system relies on the precision and the accuracy of its own localization but also on a variety of sensors: cameras, sonar, inertial unit and many more instruments used for data collection and surrounding awareness.

Very often, an AUV has to both navigate and communicate with a platform, such as a beacon, submerged instrumentation or another AUV. Since AUV mission scope are wide in term of depth or travelled distance, underwater communication ranges are from 1 centimeter to few kilometers in shallow water. Thus, neither optical or radio-frequency systems are suitable

since radio waves are confronted to a strong attenuation in salt water ( $\approx 1800$  dB/m). Therefore, radio systems such as Global Navigation Satellite System (GNSS) or cellular networks, cannot be used. Waves at visible light frequencies can reach great range, up to 100 meters but requires alignment between the optical modem of the AUV and the beacon. Underwater Acoustic (UWA) channel is therefore the privileged option for communication thanks to its better data rate versus range performance compared to others links. In the current paper, we consider conventional UWA communication scheme to do an accurate positioning.

UWA physical channels are characterized by high latency (due to sound speed of approximately 1500 m/s), low data rate (about 40 kbps  $\times$  km) and multi-path phenomenon that exhibits significant technical challenges [1].

### A. State of art on underwater positioning

In this paper, we are developing a new localization method previously introduced in [2] and [3]. The scientific community has researched on stable AUV localization techniques, leading to several innovative technologies in this domain, described in [4] and [5].

In the industry field, positioning solution for AUVs are approved. Two main technologies are the most used, that can be combined together. Having a pressure sensor and a sound velocity sensor is however mandatory. They are described as follow :

- Transponder-based systems : Single or multiple beacons sends a periodic acoustic ping or communication. This way, an estimation of the distance between the beacon and the AUV (or triangulation when at least 3 beacons are emitting) can be extracted. When beacon has multiple transponder, an estimation of the bearing angle of the communication can be made. The well know systems using these methods are Range-Only Single Beacon

(ROSB), Long Baseline (LBL), Short Baseline (SBL) and Ultra Short Baseline (USBL).

These systems provide accurate and stable localization estimation for the AUV, given by an estimation algorithm such as a Kalman filter. However they requires calibration, sound speed information and fixed localized infrastructures, which reduces flexibility and increases the deployment time depending of the number of infrastructure.

- Proprioceptive sensors (or dead-reckoning): These are Doppler Velocity Log (DVL), to compute velocity, and inertial (Inertial Measurement System (INS) or Attitude Heading Reference System (AHRS)) to compute acceleration, angular velocities, orientation, heading of the AUV. DVL are acoustic and inertial unit commonly Fiber Optical Gyroscope (FOG) but in some cases MicroElectroMechanical Systems (MEMS) [6].

AUVs always include one of these two technologies or both, since they can guarantee satisfactory localization performance. However, proprioceptive sensors requires a lot of space inside the AUV, are fairly expensive and can drift severly over time. Transponder-based systems, except for USBL and ROSB need multiple transponder architecture to deploy by its definition.

When these technologies are combined, they can enhance overall accuracy, precision and also correct each others imperfections (such as said before, drift and noises). Initialization is made through GNSS surface measurement. Kongsberg [7], Sonardyne [8] and iXblue [9] are industrial leaders of the field.

We can cite alternative methods proposed in the literature which are, e.g., in [4] Simultaneous Localization And Mapping (SLAM) with Extended Kalman Filter (EKF) [10] [11], collaborative positioning [12], and Virtual-LBL [13]. A previous work about using Doppler shift estimation to enhance AUV localization was made in [14] but with multiple hydrophones and bearing angle estimation.

### B. Underwater acoustic communication channel

UWA communications benefits compared to other underwater communication technologies are long range communication, no line of sight constraints, and cost-effectiveness. However, the UWA channel induces well known constraints. Underwater sound propagation speed is relatively low, around 1500 m/s. The time travel of each sound wave should be taken into account. One difficulty that an AUV faces is determining the Doppler scaling factor, which is related to the change in frequency caused by the movement of the transmitter with respect to the receiver called Doppler-shift. In some cases, underwater acoustic communication systems may encounter Doppler spreading, which occurs as a result of fluctuations in the scattering of acoustic waves that reach a moving surface or due to variations in the conditions of the seafloor in different locations. The Doppler scaling factor, which is proportional to the relative velocity between transmitter and receiver, has to be estimated and compensated by the decoder (receiving side) in order to compute the information bits [1]. In this paper,

we propose to use into the localization algorithm the time of flight and relative velocity estimations provided by UWA data frame synchronization and Doppler scaling factor estimation. This approach is measured experimentally and compared in the same conditions to a standard ROSB localization.

### C. Motivation

Papers [2] and [3] are previous work of respectively simulation and pool-test of this novel technique. We then spread out our work on this subject by making an experimentation on short mission trajectories in a real sea environment to examine its performance. Therefore, the proposed positioning system integrates a Doppler velocity estimation given by the single transponder communication system, distance estimation using time travelled by the UWA and inertial heading angle. As stated in section I-A, there are several methods available, and the choice of which to use depends on the specific requirements, budget, and mission specifications. One alternative to the suggested system is to estimate the projected velocity using a DVL. However, the proposed solution recommends using the Doppler relative velocity estimated by the communication system instead, which offers a simpler solution for an AUV that already has a UWA communication system, rather than having to integrate an additional DVL.

This experiment consists of a boat following very typical trajectories on the AUV field (e.g. survey path, turn around) around a geo-referenced buoy equipped with a subsea acoustic transmitter sending periodically UWA data to the hydrophone of the boat. Each acoustic instrument are submerged with a constant depth around 2-3 meters. The trials took place in the roadstead of Brest, France, in July 2022. The GNSS is used for initialization, heading angle and of course comparison to the the ground truth. The performance of our algorithm is analyzed in terms of positioning error and in comparison to standard ROSB method. The central focus is to accurately estimate the position of the boat (the imagine of the AUV) relative to the fixed buoy without any DVL speed, FOG inertial and bearing angle information.

The rest of this paper is structured as follows: In Section II, we outline the communication system model that includes both the transmitted signal and receiver algorithms. In Section III, we describe the dynamic model that was used in our experiments, and the results obtained from these experiments are presented, compared and discussed in Section IV. Finally, Section V contains the concluding remarks for this paper.

## II. COMMUNICATION SYSTEM MODEL

### A. UWA modulation

Information is transmitted by using an identical signal as in [2]. Each communication pattern is assembled with pilot symbols used for UWA channel estimation and Binary Phase Shift Keying (BPSK) data symbols carrying the information. They are pulse-shaped with a square-root raised cosine (SRRC) filter and then transposed around  $f_0 = 28$  kHz in the band between 22 kHz and 34 kHz. A pure tone signal around  $f_{pt} = 20$  kHz

is added to the useful signal in order to estimate accurately the motion induced Doppler shift [15]. The Power Spectral Density (PSD) of the transmitted signal is showed in Fig. 1.

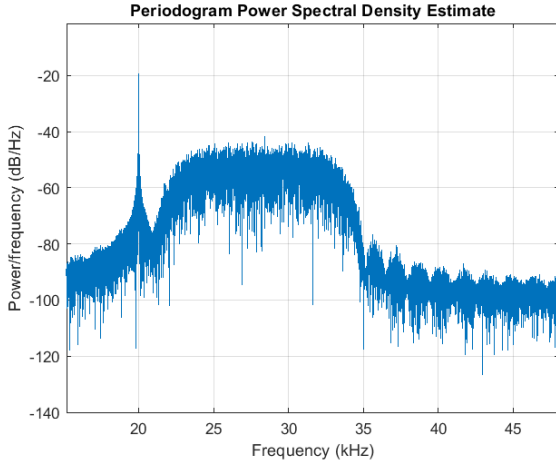


Fig. 1: PSD of the transmitted UWA communication signal.

We chose to send the communication every 3 seconds from the beacon to the boat. Since we use one way travel propagation time computation thanks to the GNSS Pulse Per Second (PPS) synchronization, this offer a theoretical range up to 4.5 kilometers. Using classical transponders having Time Difference Of Arrival (TDOA) technology, the travel is two way and then divide by two this theoretical range. As we will see in the result section, the more communication data is provided to the AUV, the more precise the positioning will be. On the other side, computational time is important, up to 1 second, and must to be taken into consideration for practical implementation.

### B. Demodulation process

The demodulation process, carried out on the AUV side, requires an estimation of the instantaneous Doppler shift and time synchronization. Our algorithm extracts the Doppler shift either from the phase derivative of the pure-tone base-band signal  $\tilde{r}_{pt}(t)$  or by successive bank of different correlations to find the best one from the filtered signal, without  $\tilde{r}_{pt}(t)$  [16]. The first method is employed by computing the phase angle from two successive samples as follows:

$$\hat{v}_r(kT) = \frac{c_w}{2\pi T f_{pt}} \arg(\tilde{r}_{pt}(kT)\tilde{r}_{pt}^*((k-1)T)) \quad (1)$$

where  $c_w$  is the celerity of sound underwater,  $T$  is the modulation symbol duration and  $\hat{v}_r(kT)$  is the estimated Doppler velocity. The other one consist of a first approximation of the Doppler induced by making correlations between received signal and dopplerized pilot symbols. When the approximation is made, a fine tune is then accomplish with dichotomy.

The distance between beacon and AUV is estimated through the frame synchronization algorithm that realizes a cross-correlation between the received signal and the known transmitted pilot symbols, with Doppler previously compensated. By assuming identical sampling frequency and sound velocity estimation, the distance is then evaluated according to the time of flight of the transmitted signal.

### III. DYNAMIC MODEL

The experiment consists of an human controlled boat with submerged hydrophone to reproduce the behavior of an AUV. In this section, whilst describing the model of an AUV, we will use this model for the boat. We assume that the AUV has a position  $(x, y)$ , the distance between buoy and AUV  $d$ , a projected velocity  $v_p$ , a relative velocity  $v_r$  from the direction AUV - Buoy, a heading angle  $\theta_h$  and finally a bearing angle  $\theta_b$  giving the  $v_r$  direction. Let us summarise each variable either it is an estimation or a measurement in Table I.

Parameters	Description	Provider
$v_p$	Projected (or real) velocity	Estimated by the Kalman Filter
$v_r$	Relative velocity	Estimation from the UWA
$\theta_h$	Heading angle of the AUV	Measured from the GNSS
$d$	Distance between acoustics	Estimation from the UWA
$\theta_b$	Bearing angle of the UWA communication	Estimated by the Kalman Filter

TABLE I: Design description

The vehicle is controlled by acceleration and rotational speed considered here unknown but that could be measured through an Inertial Measurement Unit (IMU). The buoy, reference anchor, is fixed with known  $(x_{ref}, y_{ref})$ . Our study is limited to a two-dimensional space, as we can incorporate the third dimension by taking into account the measurements from pressure sensors. The algorithm is updated each  $\Delta_t$ . In simulation, we set this value to the heading angle  $\theta_h$  measurement frequency. Due to the fact that we are using the heading angle from the GNSS in this experiment,  $\Delta_t$  is set to 1 Hz.

#### A. State space model

The state vector is defined by  $\mathbf{z} = (x \ y \ \theta_h \ v_p)^T$ , the observation vector by  $\mathbf{y} = (d \ \theta_b \ v_r)^T$

The state (2) and observation (3) equations at state  $k$  are expressed as:

$$\mathbf{z}_k = f(\mathbf{z}_{k-1}) \quad (2)$$

$$\mathbf{y}_k = g(\mathbf{z}_k) \quad (3)$$

$k$  represents the sample index of each iteration, therefore it is a natural number from 1 to the total duration of the mission  $t_{max}$ . The state (4) function and two observation (5) functions are defined by :

$$\mathbf{f}(\mathbf{z}_k) = \begin{pmatrix} x_k + v_{p_k} \cos(\theta_{h_k}) \cdot \Delta_t \\ y_k + v_{p_k} \sin(\theta_{h_k}) \cdot \Delta_t \\ \theta_{h_k} \\ v_{p_k} \end{pmatrix}^T \quad (4)$$

$$\mathbf{g}_{\text{com}}(\mathbf{y}_k) = \begin{pmatrix} \sqrt{(x - x_{\text{ref}})^2 + (y - y_{\text{ref}})^2} \\ \theta_{h_k} \\ -v_{r_k} \cos(\arctan(y - y_{\text{ref}}, x - x_{\text{ref}}) - \theta_{h_k}) \end{pmatrix} \quad (5)$$

$$\mathbf{g}(\mathbf{y}_k) = \theta_{h_k}$$

$\mathbf{g}_{\text{com}}$  is the observation function when an acoustic communication is detected and  $\mathbf{g}$  the rest of the time. When inertial unit is present inside the AUV, is it common to update the algorithm with angle velocity, accelerations and gyroscope [6]. We get the third row of (5) by applying the dynamic showed in Fig. 2 and knowing these equations :

$$\theta_b = \arctan(y - y_{\text{ref}}, x - x_{\text{ref}}) \quad (6)$$

$$v_r = v_p \cos(\theta_b - \theta_h) \quad (7)$$

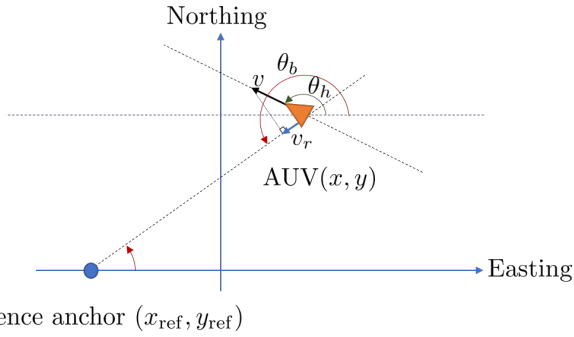


Fig. 2: Reference map of the model.

It is important to note that an estimation of the bearing angle  $\theta_b$  from the UWA communication is impossible since at least 3 hydrophones are needed to make an accurate estimation. This solution is provided by a USBL positioning technique. When comparing to ROSB solution, we avoid using any  $v_r$  estimation and then  $\theta_b$  estimation.

### B. Estimation filter

An estimator is responsible for assessing the position at a certain step with limited measurements. The EKF is the most widely used estimator in localization techniques. In a study by [17], the authors compared the performance of various localization methods in a dynamic environment using EKF, Unscented Kalman Filter (UKF), Particle Filter (PF), and Maximum A Posteriori (MAP) with range-only measurements and a single beacon. In this current study, we will be using an EKF algorithm as described in [18]. The state transition matrix, independent from  $k$ , is defined by

$$\mathbf{A} = \left. \frac{\partial f(\mathbf{z}_k)}{\partial \mathbf{z}} \right|_{\mathbf{z}_k} = \begin{pmatrix} 1 & 0 & -v_p \cdot \Delta_t \cdot \sin(\theta_h) & \Delta_t \cdot \cos(\theta_h) \\ 0 & 1 & v_p \cdot \Delta_t \cdot \cos(\theta_h) & dt \cdot \sin(\theta_h) \\ 0 & 0 & 1 & 0 \\ 0 & 0 & 0 & 1 \end{pmatrix} \quad (8)$$

The observation transition matrix is

$$\mathbf{H} = \left. \frac{\partial h(\mathbf{z}_k)}{\partial \mathbf{z}} \right|_{\mathbf{z}_k} = \begin{pmatrix} 0 & 0 & 1 & 0 & 0 & 0 \\ A \cdot (x - x_{\text{ref}}) & A \cdot (y - y_{\text{ref}}) & 0 & 0 & 0 & 0 \\ B \cdot (y - y_{\text{ref}}) & -B \cdot (x - x_{\text{ref}}) & v \sin(C) & \cos(C) & 0 & 0 \end{pmatrix} \quad (9)$$

With

$$A = \frac{1}{\sqrt{(x - x_{\text{ref}})^2 + (y - y_{\text{ref}})^2}}$$

$$B = \frac{v \sin(\arctan(y - y_{\text{ref}}, x - x_{\text{ref}}) - \theta)}{\sqrt{(x - x_{\text{ref}})^2 + (y - y_{\text{ref}})^2}}$$

$$C = \arctan(y - y_{\text{ref}}, x - x_{\text{ref}}) - \theta$$

### C. Conditions of experiment

The experiment took place at the bay of Brest in the 5th and 6th of July 2022. Since the positioning is post-processed, everything was setup such has measurements are data-logged and synchronized over PPS. While moving with a zodiac boat with one hydrophone submerged, we recorded the two GNSS signals (boat and beacon), the hydrophone signal and lastly measurements from an IMU. Despite that IMU integration was planned for the positioning estimation algorithm similarly as state-of-art, the instrument gave erroneous measures. We are then using the GNSS heading estimation for the rest of the paper. Fig. 3 shows the fixed beacon integrated with a single acoustic transmitter at a depth of 3 meters. Sound speed velocity was measured each hours through Sound Velocity Probe (SVP) instrument. The measured value was constant between 1512 and 1513 m/s for the two days.

A total of twenty trajectories of duration from 2 minutes to 15 minutes was recorded. In this paper, we chose to focus on 4 very different kind of trajectories. #1 is a 10 minutes long complex route with many U-turn but close to the beacon. #2 is a 5 minutes simple and close route. #3 is a 10 minutes long survey path going further and further away from the beacon. #4 is a 450 meters away simple path for 3 minutes and 20 seconds. Fig. 4 represents the GNSS positioning values of the first trajectory.



Fig. 3: Fixed beacon hosting the UWA transmission system.

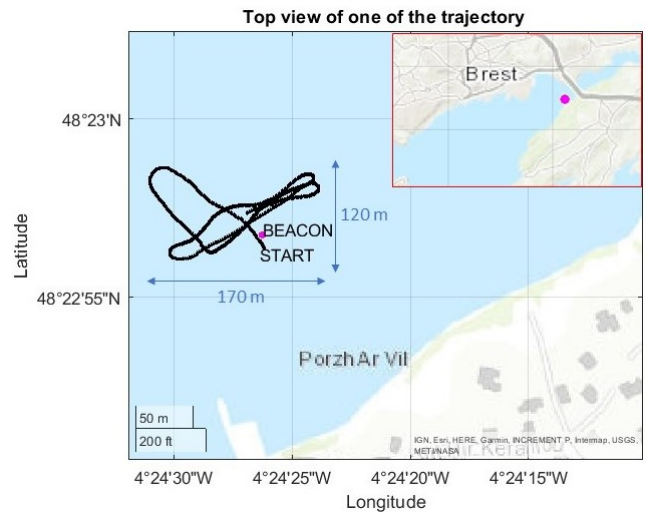


Fig. 4: Map of the trajectory #1 made by the boat.

## IV. EXPERIMENTAL RESULTS

### A. Experiment parameters

The GNSS speed of the boat was set to be between 1 knot to 6 knots. The sea current was not measured but it is estimated that it was at least 2 knots. As previously defined, the fixed beacon emit a UWA communication every 3 seconds over PPS. At initialization, the EKF is feeded with GNSS measurement. No GNSS fix is made over the trajectory.

The covariance error matrices of the EKF  $\mathbf{Q}$  and  $\mathbf{R}$  and  $\mathbf{P}_0$  are defined as follows:

$$\begin{aligned} \mathbf{Q}_k &= \Delta_t^6 \cdot \mathbf{I}_4, \\ \mathbf{R}_k &= \beta \cdot \mathbf{I}_3, \\ \mathbf{P}_{0k} &= \mathbf{I}_4. \end{aligned} \quad (10)$$

$\mathbf{P}_{0k}$  is the initial state covariance matrix of the EKF,  $\mathbf{Q}_k$  is the covariance of the process noise and  $\mathbf{R}_k$  is the covariance of the observation noise [18].  $\beta$  is a vector related to the noises of  $y_k$ . It is then varying depending of the expected noises, its values are between 0.1 to 4 on each observation.

### B. Results

Figures 5 shows the four trajectories chosen for this paper. The blue dashed line represent the ROSB state-of-art positioning estimation whereas the red dotted line represent the positioning algorithm of this article. Every routes start at (0, 0) and the known position of the buoy is represented in a red star. Real position is the GNSS measurement.

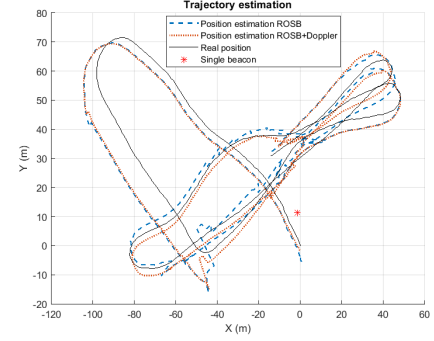
Figures 6 exhibits the positioning error and Root Mean Square Error (RMSE) over time for each trajectories. The RMSE is the image of the confidence of the EKF estimation. Finally, the table II is the summary of the results. First column is the mean of the positioning error in meter for  $v_r$  estimation with computational efficient pure-tone extraction such as described in section II. Second column is the same but with the previously exposed Doppler filter bank of correlation. Last column is the state-of-art ROSB estimation without  $v_r$  and  $\theta_b$ . Each one of the showed trajectory has a mean positioning error, compared to the GNSS, below 6 meters. This is an affirmation that can be extended to the whole sessions of experimentation regardless of the distance or the complexity of the followed route. However, we can observe that simpler path is obviously easier to estimate (such as #2) and better closer than further (#2 better than #4). Fig. 6 highlight the fact that after 10 minutes of localization, the error does not grow and thus, the algorithm does not diverge. The error mainly increases during turns for few reasons :

- The sea current imply a boat drift which impact the heading angle, bearing angle and then relative speed  $v_r$ .
- The bearing angle is not measured or estimated through UWA but through EKF linearity.
- Between each communication, the EKF only measure the heading angle  $\theta_h$ .

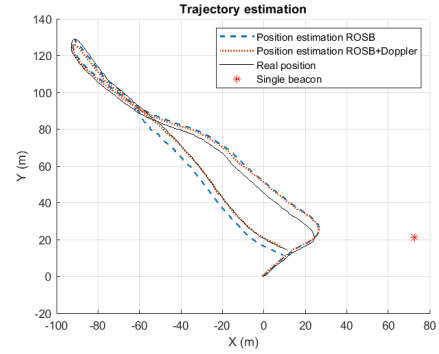
As we can see, results between pure-tone Doppler estimation and filter bank Doppler estimation are close except for the last trajectory. This can be explained by some outliers existing in the Doppler estimation.

## V. CONCLUSION

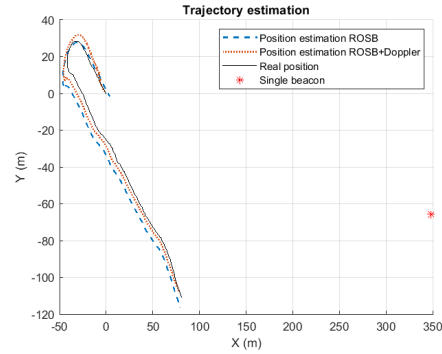
This paper provides a sea experimentation of an innovative localization approach using cost-effective Doppler shift estimation, which is computed after receiving a UWA communication. By getting the Doppler shift, we can determine the relative speed of the AUV. In comparison to the traditional method of beacon range localization, we conducted an experiment to analyse the performance of this proposed approach. In sea environment, with 3 meters depth hydrophones, we



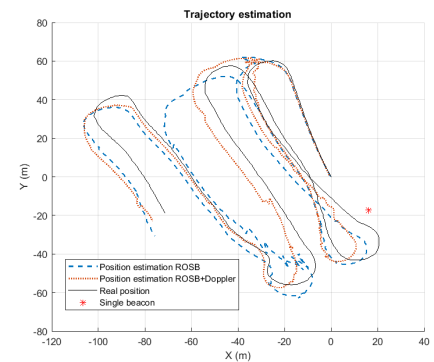
(a) Trajectory #1.



(b) Trajectory #2.



(c) Trajectory #3.



(d) Trajectory #4.

Fig. 5: Trajectories positioning estimation.

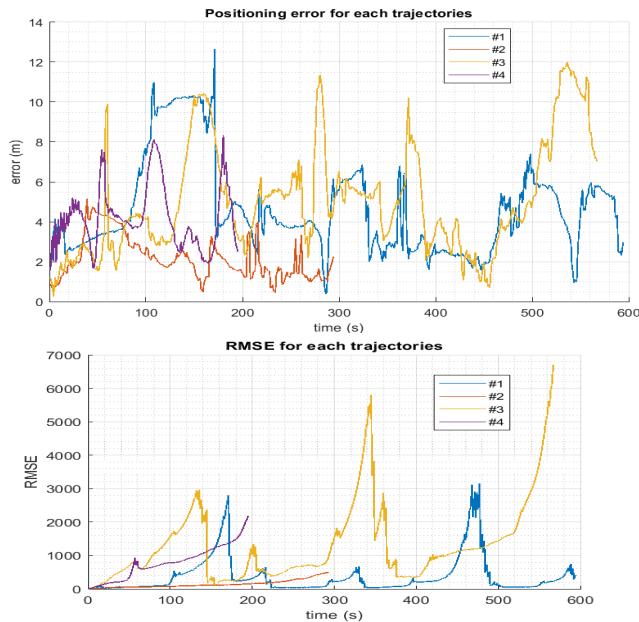


Fig. 6: Representation of positioning error error dispersion (RMSE).

Trajectory number	MPE with $r_{pt}$	MPE with filter bank	MPE for ROSB
#1 ( $t_{max}=600s$ )	4.6225 m	4.7563 m	5.4287 m
#2 ( $t_{max}=300s$ )	2.1537 m	1.9731 m	2.9931 m
#3 ( $t_{max}=600s$ )	5.0740 m	5.1593 m	8.6719 m
#4 ( $t_{max}=200s$ )	4.2069 m	5.804 m	6.2746 m

TABLE II: Result summary table. MPE for Mean Positioning Error.

showed that using Doppler shift estimation improves the localization estimation of the AUV by increasing overall accuracy compared to ROSB state-of-art. In addition, we demonstrated that with a very simple architecture, positioning approximation is possible and then small AUV navigation can be considered. Future work will focus three dimensional positioning with inertial unit measurements.

## REFERENCES

- [1] M. Stojanovic and P.-P. J. Beaujean, "Acoustic Communication," in *Springer Handbook of Ocean Engineering*, M. R. Dhanak and N. I. Xiros, Eds. Springer International Publishing, 2016, pp. 359–386.
- [2] C. Aubry, P. Forjonel, P. Bouvet, A. Pottier, and Y. Auffret, "On the use of doppler-shift estimation for simultaneous underwater acoustic localization and communication," in *OCEANS 2019 - Marseille*, pp. 1–5.
- [3] R. Garin, C. Vanwysberghe, P. Forjonel, B. Tomasi, and P.-J. Bouvet, "Simultaneous underwater acoustic localization and communication: an experimental study," in *OCEANS 2021: San Diego – Porto*, 2021, pp. 1–6.
- [4] J. González-García, A. Gómez-Espinosa, E. Cuan-Urquizo, L. G. García-Valdovinos, T. Salgado-Jiménez, and J. A. E. Cabello, "Autonomous underwater vehicles: Localization, navigation, and communication for collaborative missions," *Applied Sciences*, vol. 10, no. 4, 2020. [Online]. Available: <https://www.mdpi.com/2076-3417/10/4/1256>
- [5] H.-P. Tan, R. Diamant, W. K. G. Seah, and M. Waldmeyer, "A survey of techniques and challenges in underwater localization," vol. 38, no. 14, pp. 1663–1676, 2021. [Online]. Available: <https://www.sciencedirect.com/science/article/pii/S0029801811001624>
- [6] L. Paull, S. Saeedi, M. Seto, and H. Li, "AUV navigation and localization: A review," vol. 39, pp. 131–149.

- [7] Kongsberg website. [Online]. Available: <https://www.kongsberg.com/>
- [8] Sonardyne website. [Online]. Available: <https://www.sonardyne.com/>
- [9] Ixblue website. [Online]. Available: <https://www.ixblue.com/>
- [10] D. Lee, D. Kim, S. Lee, H. Myung, and H.-T. Choi, "Experiments on localization of an auv using graph-based slam," in *2013 10th International Conference on Ubiquitous Robots and Ambient Intelligence (URAI)*, 2013, pp. 526–527.
- [11] P. Newman and J. Leonard, "Pure range-only sub-sea slam," in *2003 IEEE International Conference on Robotics and Automation (Cat. No.03CH37422)*, vol. 2, 2003, pp. 1921–1926 vol.2.
- [12] A. Caiti, V. Calabrò, T. Fabbri, D. Fenucci, and A. Munafò, "Underwater communication and distributed localization of auv teams," in *2013 MTS/IEEE OCEANS - Bergen*, 2013, pp. 1–8.
- [13] C. E. G. LaPointe, "Virtual Long Baseline (VLBL) Autonomous Underwater Vehicle Navigation Using a Single Transponder," p. 94.
- [14] R. Diamant, L. M. Wolff, and L. Lampe, "Location tracking of ocean-current-related underwater drifting nodes using doppler shift measurements," vol. 40, no. 4, pp. 887–902, conference Name: IEEE Journal of Oceanic Engineering.
- [15] P. Kathirolu, P.-P. J. Beaujean, and N. Xiros, "Source speed estimation using a pilot tone in a high frequency acoustic modem," in *OCEANS'11 MTS/IEEE KONA*, 2011, pp. 1–8.
- [16] J. Trubuil and T. Chonavel, "Accurate doppler estimation for underwater acoustic communications," in *2012 Oceans - Yeosu*, 2012, pp. 1–5.
- [17] I. Masmitjà Rusiñol, "Acoustic underwater target tracking methods using autonomous vehicles," accepted: 2020-03-23T01:01:02Z Publisher: Universitat Politècnica de Catalunya. [Online]. Available: <https://upcommons.upc.edu/handle/2117/180789>
- [18] Y. Kim and H. Bang, *Introduction to Kalman Filter and Its Applications*, 11 2018.